

Observation of McMillan-Rowell like oscillations in underdoped YBCO junctions oriented along the node of the d-wave order parameter

L. Shkedy, P. Aronov, G. Koren and E. Polturak

*Physics Department, Technion - Israel Institute of Technology Haifa, 32000, ISRAEL**

(Dated: November 8, 2018)

Dynamic resistance spectra of ramp junctions made of underdoped $YBa_2Cu_3O_y$ electrodes and Ga-doped YBCO barrier are reported. Series of equidistant peaks were observed in these spectra in junctions oriented along the node direction. Junctions with different barrier thickness d_N , showed that the distance between adjacent peaks scales inversely with d_N . The peaks were thus identified as due to McMillan-Rowell like oscillations in the barrier. Analysis of the series of peaks yields an upper limit of about 3.7 meV on the value of the energy gap along the node. We attribute this small gap to the *is* component of the order parameter of underdoped YBCO near the interface of the junctions.

INTRODUCTION

The fine details of the symmetry of the order parameter in the high temperature superconductors (HTS) are still under debate. Determining the exact symmetry could be important for understanding the mechanism of the high T_c superconductors. Several experiments show that the dominant component of the order parameter in the HTS materials has a $d_{x^2-y^2}$ -wave symmetry, as summarized in a review article by Tsuei and Kirtley.[1] Other experiments are consistent with the existence of an additional sub-dominant component on the surface of the HTS, of *is* or id_{xy} nature.[2, 3, 4, 5, 6] Tunneling measurements of underdoped junctions show that in addition to the $d_{x^2-y^2} + is$ gap, a large gap which can be attributed to the pseudogap is also present.[7, 8, 9] The magnitude of the *is* component in these studies,[2, 3, 4, 5, 6] was found to be in the range of 1-3 meV as determined from the peak to peak distance in the conductance curves. Recent self-consistent calculations using Bogoliubov-DeGennes type equations, led to a good fit of the data assuming a pure d-wave symmetry in the bulk, and coexisting $d_{x^2-y^2}$ and *is* order parameters near the interface.[10] The magnitude of the *is* gap resulting from these simulations is 2.6 ± 0.1 meV. In the present experiment we observed series of geometrical resonances in the dynamic resistance spectra of node junctions. From these series, we find an upper limit of 3.7 meV on the energy of the sub-dominant s-wave component of the gap, which is consistent with the simulations results.

EXPERIMENTAL

The junctions used in the present study are of the same type of ramp junctions used before,[5, 6, 9, 11, 12] but instead of the Fe-doped YBCO barrier, we used a Ga-doped YBCO barrier. This was done in order to check if the appearance of the s-wave component depends on the nature of the barrier. In particular, the possible presence of magnetic impurities in the Fe doped

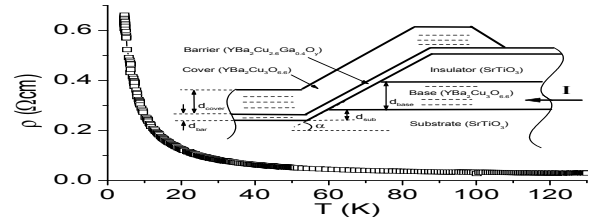


Fig. 1

FIG. 1: Resistivity versus temperature of a Ga-doped YBCO film. The resistivity values were obtained by averaging over six microbridges which were patterned in the 80 nm thick film. The inset shows a schematic cross section of a ramp type junction. The tunneling current flows along the a-b plane, while c-axis current is suppressed in the junction due to the thick insulating STO layer.

barrier, is probably absent when a Ga doped barrier is used. Therefore, observation of a signature of an *is* gap, in both type of junctions, is indicative that magnetic effects in the barrier are not likely to be the source of this gap. Fig. 1 shows the resistivity versus temperature of a blanket $YBa_2Ga_{0.4}Cu_{2.6}O_y$ film deposited on (100) $SrTiO_3$ (STO) wafer, annealed *in-situ* under the same annealing conditions as for obtaining YBCO films with $T_c = 60K$. This barrier material behaves like a Mott insulator (MI) with variable range hopping (VRH) in 3D with $\lg(\rho) \propto T^{-1/4}$ for the whole temperature range. The resistivity value at 2K is of about $0.6\Omega cm$, which is more than an order of magnitude higher than that of $YBa_2Fe_{0.45}Cu_{2.55}O_y$ used previously as the barrier layer.[12] The geometry of the junction is described schematically in the inset of Fig. 1. All the YBCO and doped YBCO layers are epitaxial with the *c* - axis

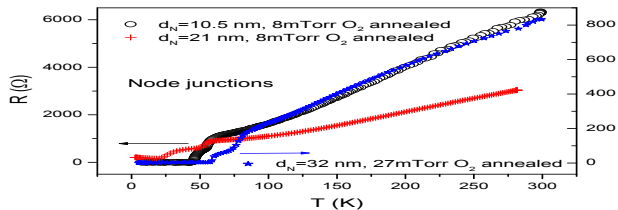


Fig. 2

FIG. 2: Resistance versus temperature of three ramp junctions with 10.5, 21 and 32 nm thick Ga-doped YBCO barrier, annealed in 8, 8 and 27 mTorr of oxygen pressure, respectively. The three junctions were patterned along the node direction at an angle of 45° to the main axis. The junction with the 10.5nm thick barrier had longer leads which led to a higher normal resistance.

normal to the wafer. The two superconducting YBCO electrodes are coupled in the $a - b$ plane via a thin barrier layer of the Ga-doped YBCO film.

The multi-step junction preparation process was described before.[11] Briefly, we first prepared by laser ablation deposition the base electrode which was composed of a bilayer of STO on YBCO on (100) STO wafer. Patterning of the base electrode was done by photolithography and Ar ion beam milling. The ramps of the junctions were patterned along the node direction of the YBCO film. After a thorough cleaning process, the cover electrode was deposited. This included the barrier layer, a second YBCO film, and an Au layer on top. The cover electrode was then patterned to produce the final junction layout, as well as the four gold pads for each junction. All junctions in the present study had the same 90nm thick YBCO electrodes (base as well as cover), the same lateral width of $5 \mu m$, and varying barrier thickness. The resistance versus temperature of the junctions was measured using the standard four probe technique, and the dynamic resistance was measured using a standard ac modulation technique.

RESULTS AND DISCUSSION

Fig. 2 shows the measured resistance as a function of temperature of three node junctions with 10.5, 21 and 32 nm thick barriers. The first two junction were annealed in 8 mTorr of flowing oxygen, and the last one in 27 mTorr oxygen flow, respectively. The corresponding normal state resistance of these three junctions is typical of underdoped $YBa_2Cu_3O_y$ with $y \sim 6.55$ for the low

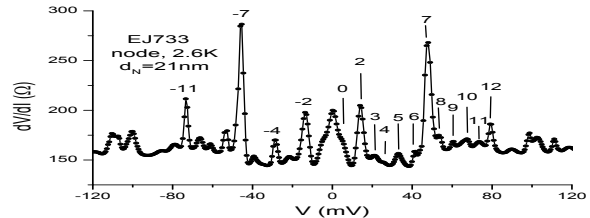


Fig. 3

FIG. 3: Dynamic resistance spectra of the junction in Fig. 2 with the 21 nm thick barrier and 8 mTorr oxygen annealing pressure.

oxygen annealed ones and $y \sim 6.85$ for the richer oxygen junction.[13] We note that the higher normal state resistance of the junction with the thinnest barrier is due to its longer leads (a different photolithographic mask pattern was used). One can observe two distinct transitions in the resistance of each junction. In the two oxygen deficient junctions (8 mTorr annealing), the transition temperature T_c of the electrodes occurs at approximately 55K, while in the third oxygen rich junction (27 mTorr annealing) the electrodes become superconducting already at 80K. The transitions seen at 40 and 25K in the first two junctions, and at 60K in the third one, result presumably from an apparent proximity effect in the barrier of the different junctions. At low temperatures, the junction with the 10.5nm thick barrier shows a critical current of about 0.5mA at 5K which yields a critical current density of $\sim 1.1 \times 10^4 A/cm^2$. The other two junctions with the 21 and 32nm thick barriers are resistive at low temperatures and have resistance values at low bias of about 200 and 2Ω , respectively. In these two cases, the barriers exhibit insulating behavior with the resistance either increasing slightly with decreasing temperature or staying almost constant.

The dynamic resistance spectra of the two oxygen deficient node junctions with 21 and 10.5nm thick barriers are shown in Figs. 3 and 4, respectively. The different behavior at low bias, namely tunneling like in Fig. 3, and critical current and zero bias conductance peak (ZBCP) in Fig. 4, is due to the much higher normal resistance of the first junction ($R_N(3K) \sim 200\Omega$). We prepared another node junction with a 32nm thick barrier, but annealed it in a higher oxygen pressure of 27mTorr. This was done in order to avoid a very high $R_N(5K)$, and yielded $R_N(5K) \sim 2\Omega$ (see Fig. 1).

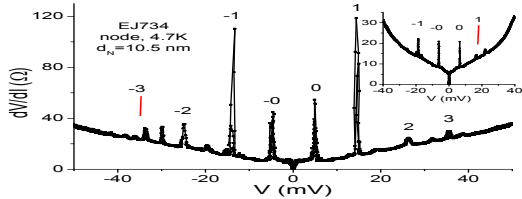


Fig. 4

FIG. 4: Dynamic resistance spectra of the junction in Fig. 2 with the 10.5 nm thick barrier and 8 mTorr oxygen annealing pressure (three traces, main panel, peak no. -3 is missing). In the inset, the results of another node junction on the same wafer are shown (two traces, peak no. 1 is missing).

The dynamic resistance spectra of this junction (not shown here) was similar to that of Fig. 3, but with a ZBCP and a more closely spaced series of peaks. In all three junctions, the position of the series of peaks on the voltage axis in the dynamic resistance curves seem to be almost independent of the oxygen content, or the presence of a ZBCP. It was however strongly dependent on the thickness of the barriers. In order to determine the origin of the series of peaks, we plotted the peak voltages versus peak number for each of the three junctions. It is generally nontrivial to associate a peak number to each peak because not all of them are present or have the same intensity. Some of the peaks are missing, some are enhanced while others can also overlap and interfere with one another. Nevertheless, by comparison with data of other node junctions, we could determine the peak numbers properly, and in Fig. 5 we plot the peak voltages of four series versus the peak number including the data of Figs. 3 and 4. Fig. 5 shows that each series of peaks appears with a constant voltage difference between adjacent peaks. Linear fits of the four series yield $V_n = 5.1 + 10.1n$ and $V_n = 6 + 12n$ for the two junctions in Fig. 4 with the thinnest barrier, $V_n = 1.9 + 6.5n$ for the junction in Fig. 3, and $V_n = 1.9 + 4.5n$ for the fourth junction with the 32nm thick barrier. The intersects at $n=0$ (5.1, 6, 1.9 and 1.9 mV) are of the same order of magnitude as the bias voltages of the corresponding first peaks in the series (5, 6, 3.4 and 2.4 mV). Fig. 5 also shows that the adjacent peaks spacing is sensitive to the barrier thickness. Its ratio in the three types of junctions is 10.1-12:6.5:4.5 which is approximately equal to the inverse ratio of the barrier thickness (1/10.5):(1/21):(1/32). Since the superconducting electrodes in all our junctions have the

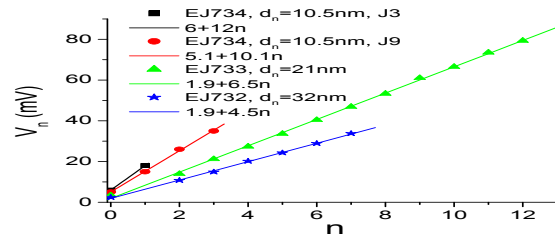


Fig. 5

FIG. 5: Peak voltages of the series in Figs. 3 and 4 versus the peak number, together with the series of peaks of the oxygen rich junction in Fig. 2 with the 32 nm thick barrier. The straight lines are linear fits to the data.

same thickness (90nm), the above result indicates that the series of peaks in the dynamic resistance spectra originate in geometrical resonances in the barrier layer. Next we discussed this result in the context of the nature of the present S/MI/S junctions (MI is Mott insulator with VRH).

It has already been demonstrated in the past that a-axis YBCO/ $PrBa_2Cu_3O_{7-\delta}$ /YBCO junctions which are basically S/MI/S junctions as we have here, carry significant critical currents I_c at low temperatures even when the barriers are up to 100nm thick.[14] Surprisingly for these kind of junctions, it was found that $I_c(T)$ behaves as $\exp[-aT^{0.5}]$ where a is a constant, which is exactly the expected behavior for SNS type junctions with a normal metal barrier in the dirty limit. There are many more reports on observations of a long range proximity effect and Andreev reflections in similar type of junctions with insulating VRH barriers.[15, 16, 17] The puzzling question is why such barrier materials with a resistivity of 0.1-1 Ωcm which is two to three orders of magnitude higher than $\sim 1m\Omega cm$ the maximum resistivity a metal can have, when in contact with a superconductor should behave like normal metals? This is a complicated problem to deal with theoretically, and only sketchy reports on this issue exist.[18] We shall not attempt to speculate here what is the reason for this normal metal like behavior of the VRH barriers in the S/MI/S junctions, but simply take it as given, and use as a first approximation the formulas derived for SNS junctions. We note however, that unlike the previous reports where the HTS electrodes of the S/MI/S junctions were close to optimal doping,[14, 15, 16] in our case the underdoped 60K YBCO based junctions yield critical current only for the thinnest 10.5nm barrier. This can

perhaps be related to the fact that the present node junctions have a weaker superconductivity coupling and shorter proximity penetration lengths, but detailed investigation of this effect is outside of the scope of the present study. We thus proceed with the treatment of our S/MI/S junctions, along the line used with SNS junctions.

We now discuss four possible types of geometrical resonances in SNS junctions that can lead to similar series of peaks in the dynamic resistance spectra like we observed here. Two are due to sub-gap scattering processes of quasiparticles, and two to above gap processes. The first two involve sub-harmonic resonances, which are caused by multiple Andreev reflections, or DeGennes-Saint James bound states.[12, 19, 20] Both result in series of peaks which are not equally spaced, and therefore are not similar to the presently observed series. Moreover, the junctions in the present study are oriented along the node direction where the d-gap vanishes, and the s-gap is too small to allow us to attribute the peaks at large voltage to sub-gap structures. The second group of scattering processes that leads to above gap series involves Tomasch and McMillan-Rowell oscillations.[21, 22] The Tomasch oscillations are due to resonances in the superconducting electrode, and their peak energies are given by

$$eV_n = \sqrt{(2\Delta)^2 + \left[\frac{nhv_{FS}}{2d_S}\right]^2}, \quad (1)$$

where Δ is the superconducting gap, v_{FS} is the Fermi velocity in the electrodes, d_S is the superconducting electrode thickness, and n is the serial number of the peak. Thus the resonances are not equally spaced, but for small energy gap values the deviation from a constant voltage difference between adjacent peaks is quite small, and generally cannot be observed due to experimental error. McMillan-Rowell oscillations (MRO),[22] are also seen as series of equidistant peaks in the dynamic resistance spectra above the gap, and are caused by geometrical resonances of quasiparticles in the barrier. The voltage difference between adjacent peaks in this series is given by

$$\Delta V = \frac{hv_{FN}}{4ed_N}, \quad (2)$$

where v_{FN} is the Fermi velocity in the barrier, and d_N is the barrier thickness. We thus find that both the Tomasch like and McMillan-Rowell like oscillations can yield the linear behavior of the peak voltage versus peak number seen in Fig. 5, provided the node gap is small compared to the adjacent peak spacing. The voltage difference between adjacent peaks however, depends on either the thickness of the superconducting electrode

in the Tomasch scenario as seen in Eq. (1), or on the barrier thickness in the MRO case as seen in Eq. (2). Since the thickness of the superconducting base and cover electrodes is the same for all our junctions, and the observed series of peaks depend on the thickness of the barrier as seen in Fig. 5, it seems that these series are due to McMillan-Rowell like oscillations. Compared to the original study of MRO,[22] the presently observed conductance peaks are much sharper, especially those in Fig. 4. As mentioned above, the linear fits in Fig. 5 show that the ratio of adjacent peaks spacing is approximately equal to the ratio of the inverse thickness of the barriers. It thus follows that scaling with the barrier thickness d_N as depicted by Eq. (2), is found here, and the observed resonances are due to McMillan-Rowell like oscillations. We stress that this result is independent of either the barrier strength or the different oxygen content of the junctions. For a normal metal barrier, Eq. (2) would have allowed us to determine also the Fermi velocity of quasiparticles in the barrier. In the present case of S/MI/S junctions with SNS like behavior, analysis yields an effective velocity $v_{FN} = 1.2 \pm 0.2 \times 10^7$ cm/sec, which compares well with a previous result of 1.5×10^7 cm/sec measured in the same kind of junction with a Fe-doped YBCO barrier. The later has a much lower resistivity value at low temperatures, of the order of $10 - 20 m\Omega cm$, thus being much closer to a normal metal than the present Ga doped YBCO. A-priori the Fermi velocity is not well defined here since there is no Fermi surface at all in isolated VRH materials. When the thin VRH layer however, is in contact with a superconductor like in the present junctions, it is possible that the Fermi surface is recovered, and the Fermi velocity is thus well defined. The fact that similar numbers were obtained for v_{FN} of the Fe and Ga doped YBCO barriers which have very different resistivity values, further supports the notion that the S/MI/S junctions have N like features. These v_{FN} values of course are only approximate ones. They are quite smaller than the value $v_F \approx 2.5 \times 10^7$ obtained by ARPES along the node direction in differently doped LSCO crystals.[23] This ARPES study also shows that there is no direct link between the measured Fermi velocity in the cuprates and the size of the resistivity.

Since the McMillan-Rowell like oscillations occur at energies above the gap, the voltage of the first peak in each series constitutes an upper limit on the magnitude of the gap energy. Previously, Neshor and Koren measured McMillan-Rowell oscillations in junctions that were directed along a main crystallographic axis of YBCO where the d-gap is at its maximum.[12] The first peak in their series appears at 16 mV, which is an upper limit on the value of the dominant d-wave component of the gap in the 55K phase of underdoped YBCO. In the present study, on the contrary, the junctions are aligned along the node direction where the dominant d-wave gap

vanishes, and we can thus measure an upper limit on the gap energy of the sub-dominant component. The first peak (knee) in Fig. 3 is found at 3.4 mV, and its voltage in Fig. 4 is 5-6 mV. This yields an upper limit on the value of the s-gap in the range of 3.4-6 meV, which is in reasonable agreement with the measured gap values of 2.5 ± 0.5 meV found previously.[5, 6] We note however, that if we take the average value of the intercepts of the four straight lines in Fig. 5, we obtain a value of 3.7 mV. This represents a four series average of the voltage of the first peak, which is thus a more reliable upper limit on the energy of the s-gap near the interface.

CONCLUSIONS

The present study shows that the experimental properties of S/MI/S junctions made of underdoped YBCO have several common features with normal SNS junctions. Measurements of dynamic resistance spectra in underdoped YBCO junctions along the node direction, show geometrical resonances in the barrier which behave like McMillan-Rowell oscillations above the gap. From these we find an upper limit of 3.7 meV on the magnitude of the *is* component of the gap near the interface.

Acknowledgments: This research was supported in part by the Israel Science Foundation, the Heinrich Hertz Minerva Center for HTSC, the Karl Stoll Chair in advanced materials, and by the Fund for the Promotion of Research at the Technion.

* Electronic address: gkoren@physics.technion.ac.il;
URL: <http://physics.technion.ac.il/~gkoren>

- [1] C. C. Tsuei and J. R. Kirtley, Rev. Mod. Phys. **72**, No 4, 969 (2000).
[2] M. Covington, M. Aprili, E. Paraoanu, L. H. Greene, F.

- Xu, J. Zhu and C. A. Mirkin, Phys. Rev. Lett. **79**, 277 (1997).
[3] R. Krupke and G. Deutscher, Phys. Rev. Lett. **86**, 4634 (1999).
[4] Sharoni A., Koren G. and Millo O., *Europ. Phys. Lett.*, **54** (2001) 675.
[5] G. Koren and N. Levy, Europhys. Lett. **59**, 121 (2002).
[6] G. Koren, N. Levy and E. Polturak, J. of Low Temp. Phys. **131**, 849 (2003).
[7] G. Deutscher, Nature **397**, 410 (1999).
[8] V. M. Krasnov, A. Yurgens, D. Winkler, P. Delsing and T. Claeson, Physica C **352**, 89 (2001), and V. M. Krasnov, A. E. Kovalev, A. Yurgens and D. Winkler, Phys. Rev. Lett. **86**, 2657 (2001).
[9] G. Koren, L. Shkedy and E. Polturak, Physica C, in press (2003). cond-mat/0306594.
[10] I. Lubimova and G. Koren, Phys. Rev. B, in press (BE9094). cond-mat/0306030 (2003).
[11] O. Neshet and G. Koren, Appl. Phys. Lett. **74**, 3392 (1999).
[12] O. Neshet and G. Koren, Phys. Rev. B **60**, 9287 (1999).
[13] Y. Ando and K. Segawa, Phys. Rev. Lett. **88**, 167005 (2002).
[14] T. Hashimoto, M. Sagoi, Y. Mizutani, J. Yoshida and K. Mizushima, Appl. Phys. Lett. **60**, 1756 (1992).
[15] U. Kabasawa, Y. Tarutani, M. Okamoto, T. Fukazawa, A. Tsukamoto, M. Hiratani and K. Takagi, Phys. Rev. Lett. **70**, 1700 (1993).
[16] C. Stozel, M. Siegel, G. Adrian, C. Krimmer, J. Sollner, W. Wilkens, G. Schulz and H. Adrian, Appl. Phys. Lett. **63**, 2970 (1993).
[17] A. Frydman and Z. Ovadyahu, Europhys. Lett. **33**, 217 (1996).
[18] Y. Tanaka, *Coherence in high temperature superconductors*, edited by G. Deutscher and A. Revcolevschi, World Scientific, Singapore (1995), pp 393-411.
[19] A. F. Andreev, Sov. Phys. JETP **19**, 1228 (1964).
[20] P. G. de Gennes and D. Saint-James, Phys. Lett. **4**, 151 (1963).
[21] W. J. Tomasch, Phys. Rev. Lett. **15**, 672 (1965); *ibid* **16**, 16 (1966).
[22] J. M. Rowell and W. L. McMillan, Phys. Rev. Lett. **16**, 453 (1966); W. L. McMillan and P. W. Anderson, Phys. Rev. Lett. **16**, 85 (1966).
[23] Z. X. Shen, cond-mat/0305576 (2003).